Technical University of Denmark

DTU

Influence of structural heterogeneity on the structural coarsening during annealing of polycrystalline Ni subjected to dynamic plastic deformation

Zhang, H.W.; Luo, Z.P.; Hansen, Niels; Lu, K.

DTU Library
Technical Information Center of Denmark

Influence of structural heterogeneity on the structural coarsening during annealing of polycrystalline Ni subjected to dynamic plastic deformation

Influence of structural heterogeneity on the structural coarsening during annealing of polycrystalline Ni subjected to dynamic plastic deformation

H W Zhang[1,*], Z P Luo[1], N Hansen[2] and K Lu[1,*]
[1]Shenyang National Laboratory for Materials Science, Institute of Metal Research, CAS, 110016 Shenyang, China
[2]Danish-Chinese Center for Nanometals, Section for Materials Science and Advanced Characterization, Department of Wind Energy, Technical University of Denmark, Risø Campus, DK-4000 Roskilde, Denmark

E-mail: hwzhang@imr.ac.cn; lu@imr.ac.cn.

Abstract. The structural heterogeneity of a polycrystalline Ni subjected to dynamic plastic deformation to a strain of 2.3 was characterized, and its influence on the structural coarsening behaviour during post annealing was investigated. Structural heterogeneity on the large scale manifests itself by formation of two types of layers: low misoriented regions (LMRs) and highly misoriented regions (HMRs). On the small scale, the heterogeneity was characterized by different distributions of boundaries and textures in each layer. LMRs contain only low angle boundaries and one dominating crystallographic orientation. In contrast HMRs contain both low and high angle boundaries (>15º) and the texture is mixed with <011> close to the compression axis. During annealing, LMRs coarsen uniformly and recrystallization nucleation is difficult to form. In HMRs, the structural evolution is heterogeneous and recrystallization nuclei are readily formed. The importance of structural heterogeneity during structural design for high performance nanostructure was highlighted.

1. Introduction

Plastic deformation of metals is intrinsically heterogeneous, and different grains or different parts of one grain are usually subjected to different deformations and in turn distinct microstructures and textures are formed [1, 2]. As is the main theme of this symposium, structural heterogeneity is of greatly scientific and technological importance in terms of the structural adjustment for property optimization in particular for nanometals with high strength but low ductility and low thermal stability.

Recently, high strain rate deformation, as has been demonstrated by dynamic plastic deformation (DPD) [3-6], has drawn increasing interest owing to the significant grain refinement down to nanometer regime as well as the novel final structures that are distinct from the low strain rate deformed counterparts. Taking polycrystalline Ni for consideration, DPD reduces the structural scale down to ~120 nm at a substantially low strain of 2.3, forming typical lamellar structure composed of 70% low angle boundaries. Comparatively, for low strain rate deformation a similar refinement effect generally requires a strain as larger as >12, and the final product is characterized by an ultrafine grained structure containing >70% high angle boundaries [7, 8]. Besides, DPD fabricates heterogeneous deformation microstructures, distinct regions are characterized by different microstructures and textures [9]. The structural coarsening behaviours of DPD Ni during post

annealing as well as the influence by the structural heterogeneity will be investigated in the present study.

2. Experimental

Table 1. Chemical compositions of the Ni samples (wt.%)

C	Si	Mn	P	S	Cr	Fe	Al	Co	Cu	Ti	Mg	Ni
0.002	0.007	0.002	0.004	0.001	0.001	0.011	0.001	0.002	0.001	0.005	0.003	99.96

A polycrystalline Ni with a purity of 99.96 wt.% (Table 1) was used as the experimental material. The starting material was fully recrystallized, with grain size ranging from 30-300 μm (an average of 100 μm), Fig. 1. Following our previous investigation [6], cylindrical Ni samples with a diameter of 20 mm and a length of 20 mm was subjected to DPD at room temperature to a strain of ε =2.3, hereafter denoted as DPD Ni. The strain is defined as the logarithm ratio of the initial height L_0 to final height L_f : $\varepsilon = \ln(L_0/L_f)$. Annealing was carried out at 100-700 °C for 1h in a quartz tube filled with Ar gas, followed by air cooling to room temperature. The microstructure at each annealing temperature was quantitatively characterized.

Figure 1. Optical microscopic image of the starting polycrystalline Ni sample.

Structural characterization was carried out on the longitudinal section that is parallel to the loading direction by a JEOL 2010 transmission electron microscope (TEM) and a FEI Nova NanoSEM 430 field emission gun scanning electron microscope (FEG-SEM). The boundary spacing of the deformation microstructure was determined by measuring, on the TEM micrographs, the interception length along lines perpendicular (D_T) and parallel (D_L) to the compression axis, respectively. The random boundary spacing (D_r) was calculated according to: D_r=2/(1/D_T+π/(2D_L)) [10]. Their boundary misorientation angles and the microtexture were measured via CBED in TEM and EBSD in SEM. The structure and texture of the annealed samples were characterized only by EBSD. The EBSD data were collected with a scanning step size of 0.1 μm and were analyzed with a HKL Channel 5 system, where boundaries that are misoriented less than 2° were excluded for the statistical analysis. The Vickers microhardness (H_V) of the as-deformed and as-annealed DPD Ni samples was measured on the longitudinal section with a load of 0.98 N and a loading time of 10 s. Each data point was averaged at least 10 measurements.

3. Results

3.1. Deformation microstructures
A boundary map reconstructed from EBSD data reveals two distinct regions in the DPD Ni, Fig. 2a. One region termed as highly misoriented regions (HMRs) is a mixture of low angle boundaries (LABs, indicated by thin green lines) and high angle boundaries (HABs, indicated by bold black lines), and the other named as low misoriented regions (LMRs) contains solely low angle boundaries. As indicated by the <110> pole figures in Fig. 2, LMRs show one single orientation, whereas HMRs contain many orientations with <110> close to the compression axis (CA), i.e. <110>fiber texture.
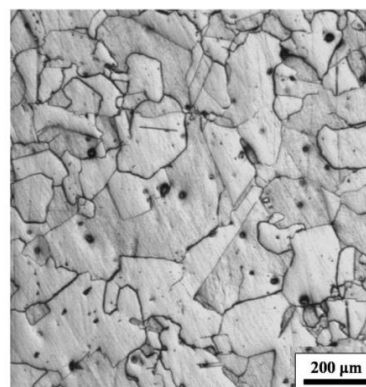
TEM observation, Fig. 2b, shows that the microstructure inside both HMRs and LMRs is a lamellar structure, which is characterized by straight and flat lamellar boundaries (LBs) bordering volumes composed of interconnecting dislocation boundaries and low densities of loose dislocations. Such microstructure is the typical microstructure developed in metals of high stacking fault energy during monotonic deformation to low-to-medium strains, where plastic deformation was accommodated by dislocation slip [1, 2, 7, 10]. However, the length of these lamellar boundaries reaches several to tens of microns, whereas the width (D_T in Table 2) is in the nanometer regime, which gives rise to an aspect ratio significantly larger than 100. D_T and D_L for HMRs (114.2 nm and 332.8 nm) are slightly smaller than those of LMRs (136.1±6.1 nm and 349.8±11.9 nm). Besides, LMRs include only LABs, whereas HMRs contain 29.8% HABs.
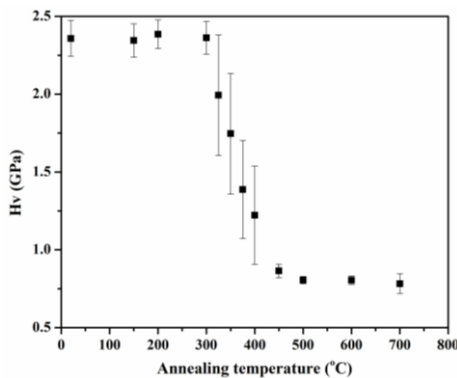

Figure 2. (a) Boundary map reconstructed from EBSD data showing two types of regions and the corresponding pole figures in DPD Ni: LMRs and HMRs. (b) TEM observation together with the boundary sketch of the lamellar structure formed in the DPD Ni. Thin green line in (a) and thin black line in (b) indicates low angle boundaries, whereas high angle boundaries are indicated by bold black lines. The compression axis (CA) was indicated by arrow.

Figure 3. Variation of hardness as a function of annealing temperature of DPD Ni.

Table 2. Boundary parameters of HMRs and LMRs

Structure	D_T (nm)	D_L (nm)	D_{av} (nm)	θ_{av} ($<15^o$)	f_{HAB} ($>15^o$)
HMRs	114.2	332.8	148.4	5.5	29.8%
LMRs	136.1	349.8	169.0	4.9	0

3.2. Annealing behavior

3.2.1. Hardness-Temperature

During annealing at temperature from 100-700°C for 1h, the hardness of DPD Ni decreases with an increase of annealing temperature, Fig. 3, exhibiting three stages: i) a slight hardness change as temperature increases up to 300°C, corresponding to a low temperature recovery; ii) a sharp drop of hardness from 2.4 to 0.9 GPa in the temperature range from 300 to 450 °C, implying a recrystallization at medium temperatures; and iii) a small decrease of hardness from 0.9 to 0.8 GPa in the temperature span of 450-700 °C, i.e. a grain growth after recrystallization at high temperature. Such hardness change with annealing temperature was also observed in a 99.967% Ni subjected to HPT to a strain of 100 [8]. However, compared with HPT Ni, the hardness change in the recovery stage for DPD Ni is less significant and the recrystallization temperature corresponding to 50% hardness drop is higher by ~200°C.
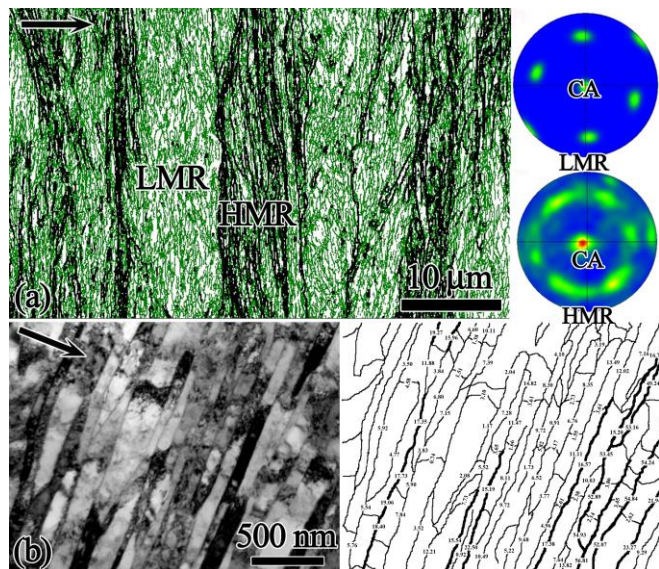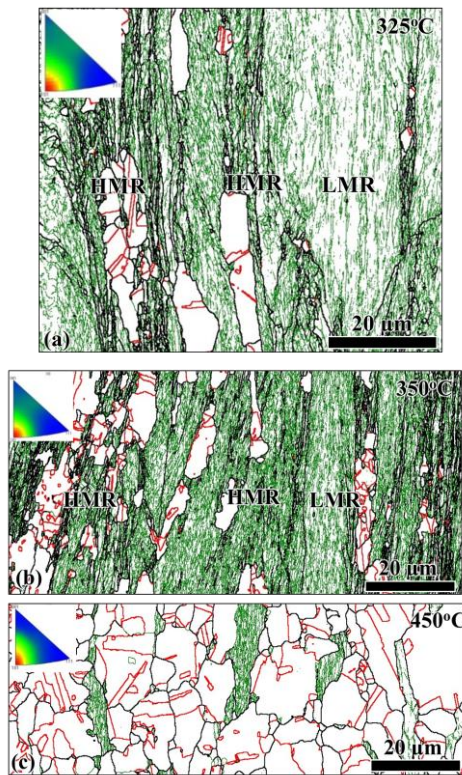
3.2.2. Microstructure-temperature

Figure 4. Boundary maps reconstructed from EBSD data of DPD Ni during annealing at different temperatures for 1h. Red lines indicate the annealing twin boundaries. Inverse pole figures are inserted.

The microstructure of the DPD Ni annealed at temperatures lower than 300ºC resembles the deformation microstructure. No apparent changes in the structural pattern and boundary parameters were detected for both HMRs and LMRs. As temperature increases up to 325ºC, Fig. 4a, LMRs remain the deformed state, however, high angle boundaries in the HMRs becomes wavy and rough. Small (nuclei) and large recrystallization grains are also observed with clean interiors bordered by high angle boundaries. These grains frequently contain annealing twins. Some grains are formed in the regions close to the interface between LMRs and HMRs, others are in the HMRs interiors. For both cases, the nucleation positions are composed of high density of high angle boundaries. Besides, the recrystallization grains are not equiaxed but extended along LBs. The longitudinal size (parallel to LB, D_L) is larger than the transversal size (perpendicular to LBs, D_L) by a factor of 1-8. As temperature increases to 350ºC, Fig. 4b, LMRs remain unchanged, while more areas in HMRs recrystallize. Nucleation takes place continuously in the clusters of high angle boundaries, which is supplemented with the concurrently growing along LBs leading to banded recrystallization regions. After annealing at 450ºC, most of the deformation matrix has been recrystallized, leaving small amount of LMRs embedded in the recrystallization grains, Fig. 4c. These recrystallization grains, however, are roughly equiaxed, though extended morphologies can still be detected in particular for small grains. It should be noted that as evidenced from the inserted inverse pole figures (IPF) in Fig. 4, <110> fiber texture was well retained even fully recrystallization has taken place.

The variation of the boundary spacing as a function of annealing temperature for both HMRs and LMRs gives rise to "S"-shape, Fig. 5. Two slightly coarsening stages observed at low temperatures (stage I) and high temperatures (stage III) are bridged by a stage with a fast increase of boundary spacing at medium temperatures (stage II). The intersection of the tangent lines of stage I and stage II points to the onset temperature for structural coarsening (T_{on}). For LMRs, the T_{on} is 410ºC, whereas for HMRs it is 360ºC. It is also found that the structural coarsening during stage II for LMRs is faster, and the final grain size is also relatively bigger.
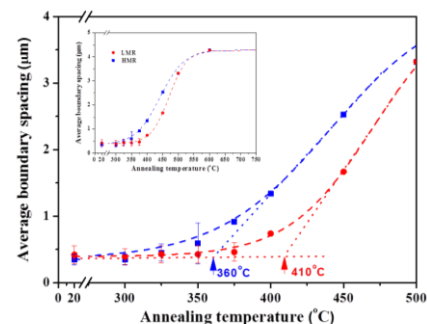

Figure 5. Variation of boundary spacing as a function of annealing temperature for HMRs and LMRs in DPD Ni.

4. Discussion

4.1. Structural heterogeneity

The deformation microstructures of DPD Ni as evidenced by both TEM and EBSD are heterogeneous. Such heterogeneity exhibits on both a fairly large scale and a small scale. Large scale heterogeneity manifests itself by the formation of two different layers defined as HMRs and LMRs, whereas the small scale heterogeneity characterizes by the difference in the structural parameters and textural components. Such structural heterogeneity has its cause partially related to the macroscopic subdivision, which has recently been found in polycrystalline copper subjected to DPD, where it was suggested that a large initial grain size (~200 μm) and different crystallographic orientations of the individual grain can result in different deformation patterns [11]. A similar dependency might result in a correlation between the scale of the macroscopic subdivision and the original grain size distribution. Assuming that the coarse grains with the grain size of 30-300 μm (average of 100 μm) are subjected to a total strain of ε=2.3 (thickness reduction of 90%), the grains would be compacted to 3-30 μm. This thickness is in accord with the layer thickness of HMRs and LMRs as shown in Fig. 2. This implies that HMRs and LMRs may be corresponding to the different original grains and their interfaces are most likely the original grain boundaries. However, it should be noted that lamellar boundary spacing for both HMRs and LMRs (136 nm for LMRs and 114 nm for HMRs) is tens to hundreds of times smaller than that of the compacted original grain boundaries (3-30 μm). This means that the original grain boundaries only account for a small fraction, whereas most of the HABs are produced by plastic deformation. That is to say HMRs and LMRs were predominately formed through the orientation splitting into different parts with distinct deformation behaviours.

The difference in structural scale and boundary distribution may lead to the difference in the stored energy that acts as the driving force for structural coarsening during post annealing. The energy can be estimated according to the structural parameters listed in Table 2. Generally, stored energy to a first approximate is contributed from elastic energy from dislocation structure and boundary energy from high angle boundaries, neglecting the contributions from vacancies and long range stress. The elastic energy (E_d) is approximated the energy per unit length of dislocation line multiplied by the dislocation density (ρ) [12]:

$$E_d = \rho \frac{Gb^2 f(v)}{4\pi} ln(\frac{R}{b}) \tag{1}$$

where G is the shear modulus (79 GPa), b is the Burgers vector (0.249 nm), v is the Poisson's ratio (0.31) and $f(v)$=(1-v/2)/(1-v), i.e. $f(v)$~1.225. R is the upper cut-off radius and is approximated by the average dislocation spacing, i.e. R~$1/\rho^{1/2}$. Generally, the loose dislocations presented in between boundaries are of the order of 10^{14}-10^{15}m^{-2}, which gives rise to a stored energy of ~0.2-2 MPa. For LABs, the stored energy can be viewed as contribution from the dislocations present in them, following *eq.* (1). The dislocation density (ρ_{LAB}) can be estimated based on the misorientation angle (θ): ρ_{LAB} =1.5$\theta S_v/b$, assuming that the boundaries are mixed boundaries [1].

The contribution from HABs (E_b) can be the product of surface area per unit volume (S_v=1/D_T+π/(2D_L)) [10] and the boundary energy per unit area (γ) [13]:

$$E_b = \gamma \cdot S_v \cdot f_{HAB} \tag{2}$$

where γ for Ni is 0.866 J/m^2 [14] and f_{HAB} is the fraction of high angle boundaries. The total contribution can be a linear additivity of E_b and Ed.

By taking the structural parameters in Table 2, the stored energy for LMRs (E_{LMR}) and HMRs (E_{HMR}) are 11.2 MJm^{-3} and 13.7 MJm^{-3}, respectively. The calculation does reflect the heterogeneous distribution of stored energy, however, the difference is not very large (~23%), which should be partially attributed to the fact that ~70% boundaries in HMRs are LABs.

Consequently, the above analysis underpins the structural heterogeneity presented in the deformation microstructures of DPD Ni, which in turn influences the structural behaviours during the subsequently annealing.

4.2. Structural coarsening

The structural coarsening of DPD Ni subjected to annealing at different temperatures shows different rates, i.e. slow coarsening during low and high temperature annealing and fast structural coarsening at medium temperatures. This is reflected by the hardness change with an increase of annealing temperature (Fig. 3), which depicts three annealing stages: recovery, recrystallization and grain growth. Such a correlation between hardness and annealing temperature has been well documented in literature [13]. However, the structural coarsening behaviours of HMR and LMR differ significantly owing to their distinct structural heterogeneity.

4.2.1 HMRs

The microstructure of HMRs coarsens in a heterogeneous manner. First of all, recrystallization nucleation takes place heterogeneously. In the sample annealed at 325°C for 1h (Fig. 4a), nucleation occurs locally in HMRs while the rest of sample remains in the deformation state. Such heterogeneous nucleation should have its cause related to its structural features. HMR contains ~30% high angle boundaries and 70% low angle boundaries. High angle boundaries, owing to the higher energy, high mobility and low activation energy, are more mobile [13]. This could be verified by the observation that local wavy and roughness appeared in the high angle boundaries in the HMRs (Fig. 4a). As triple junction migration has been proposed as an important recovery mechanism for lamellar structure composed of mainly high angle boundaries [15, 16], the presence of high angle boundaries in HMRs should have the chance of forming mobile Y-type tripe junction that is composed of three lamellar boundaries with medium to high misorientation angle [15]. Such triple junction was observed in the boundary sketch of Figure 2b, which is composed of three boundaries that are misoriented by 53.45^o, 15.2^o and 53.6^o, respectively. As a result, the readily migration of high angle boundaries together with the high mobile triple junction may be responsible for the nucleation process, which is supported by the observation that recrystallization nuclei are only observed in the places with high density of high angle boundaries.

The heterogeneous structural coarsening manifests itself also by the directional growth. As evidenced by Fig. 4, the recrystallization grains inside HMRs are hardly observed as equiaxed in shape but frequently extended along LBs. It seems that the parallel growth is more easily than perpendicular growth. Such directional growth is less apparent in the lamellar structure fabricated by cold rolling [17] and HPT [8] to large strains. The cause should be related to the heterogeneous distribution of boundary and texture in DPD Ni. DPD-induced lamellar structure in HMRs contains around 70% low angle boundaries which include both LBs and interconnecting dislocation boundaries. The LABs usually form clusters that are adjacent to those with high angle boundaries. Comparatively, for large strain cold rolled Ni [10] and high pressure torsion (HPT) deformed Ni [7, 8], lamellar structure was also fabricated but the HABs accounts for >50-60%. HABs in these samples are the lamellar boundaries but LABs are mainly the interconnecting dislocation boundaries in between LBs, and the formation of HAB clusters or LAB clusters in these samples are not observed. Besides, HMRs show <110> fiber texture, which is contributed from LAB clusters and HAB clusters. The former shows only single orientation, but the latter contains many orientations with <110> close to compression axis. The distribution of HAB clusters and LAB clusters leads to the alternatively distributed textures. On the contrary CR Ni forms rolling textures that are composed of different textural component, while HPT Ni produces shear texture that consists of different shear component. In both cases, banded regions with single orientation were not observed.

4.2.2 LMRs

With an increase of annealing temperature, the microstructures of LMRs coarsen with a uniform manner, and recrystallization nuclei were not observed even after they were consumed by the growth of recrystallization grains formed in HMRs. The uniform structural coarsening could be reflected by the roughly linear changes of boundary spacing with annealing temperature in the temperatures lower than 375°C, where the growth of recrystallization grains into LMRs is less significant (see Fig. 5). As

recrystallization grains formed in HMRs start to consume LMRs at temperature > 375°C, the linear relationship will not hold. Both the uniform structural coarsening and the difficulty in recrystallization nucleation should have their causes related to the structural and textural character. As has been evidenced by the structural characterization, boundaries including LBs and interconnecting dislocation boundaries in LMRs are low angle boundaries. Owing to the low energy, low mobility and high activation energy for boundary migration [13], the migration of such boundaries requires higher temperatures. Since all the boundaries are low angle boundaries, triple junction migration should be reduced to minimum as mobile Y-type junctions that are composed of three high angle boundaries are actually not involved in this regions. Low angle boundaries also lead to low stored energy, i.e. low driving force for boundary migration. Besides, LMRs show single orientation with small orientation spread (see Fig. 2). Under such condition, even if nucleation takes place inside LMRs, the growth into deformed matrix with similar orientation should be expected difficult owing to the orientation pinning effect [18].

4.3. Structural design
The present investigation underpins the significant influence of structural heterogeneity presented in the deformation microstructure on the structural coarsening behaviours during post annealing. Structural coarsening preferentially takes place in regions composed of different boundaries and different orientations, i.e. more heterogeneous regions. On the contrary, the regions consisting of identical structural and texture, i.e. less heterogeneous regions, are thermally more stable. With respect to the high strength but low ductility of nanometals, the necessary structural adjusting to produces so-called bi-model or multi-modal grain size distribution has significantly optimized the strength and ductility combination [19, 20]. The present investigation may provide with potential structural optimization strategy through adjusting the distribution and volume fraction of hard and soft regions by proper annealing treatment. As the structural heterogeneity has the cause related to the stability of the starting orientation, the choice of single crystallites with unstable orientations to subject to high strain rate deformation would produce also such heterogeneous structure. Under such condition, it might be possible to control the orientation splitting through adjusting the processing parameters, which in turn control the structural heterogeneity and the structural coarsening behaviour during annealing.

Besides, owing to fact that microstructures with less heterogeneity are thermally more stable. Structural design by tailoring the microstructure through such microstructure would simultaneously enhance the strength and thermal stability of nanometals. For the present case, lamellar structure composed of only low angle boundaries can be a potentially option for such purpose. Actually, recent investigation has support this hypothesis [21], where nanometre scale laminated structure with mainly low angle boundaries was fabricated in a Ni sample by means of surface mechanical grinding treatment, the hardness can be as high as 6.4 GPa that is 3 times higher than the UFG counterparts, more interestingly, the onset temperature for structural coarsening is also higher by 40K. With this purpose, single crystals with relatively stable orientation to subject to high strain rate deformation might be a choice, which is one of our on-going projects.

5. Conclusions
A polycrystalline Ni was subjected to dynamic plastic deformation to a strain of 2.3. The structural heterogeneity was examined and the influence on the structural coarsening behaviour during post annealing was investigated. The following conclusions can be reached:
1. DPD introduces a heterogeneous deformation microstructure in Ni. Low misoriented regions (LMRs) composed of only low angle boundaries coexisted with highly misoriented regions (HMRs) with a mixture of both low and high angle boundaries. LMRs show roughly a single orientation, whereas HMRs contain many orientations but with <011> close to the compression axis.

2. The structural coarsening is greatly influenced by structural heterogeneity. LMRs coarsen uniformly and formation of recrystallization nuclei is difficult. HMRs, on the contrary, show heterogeneous structural coarsening. Nucleation preferentially takes place in regions with high angle boundaries and the grain growth along LBs is faster than that perpendicular to the LBs.
3. Structural heterogeneity, being a result of plastic deformation, is shown of great importance in terms of the structural design for high performance nanostructure due to the close relationship between deformation microstructure and the nucleation and recrystallization behaviour.

Acknowledgments

Reference

[1]   Hansen N 2001 *Metall. Mater. Trans.* A **32** 2917
[2]   Huang X and Winther G 2007 *Phil. Mag.* **87** 5189
[3]   Tao NR and Lu K 2007 *J. Mater. Sci. Technol.* 23 771
[4]   Li YS, Tao NR and Lu K 2008 *Acta Mater.* **56** 230
[5]   Yan FK, Tao NR and Lu K 2012 *Acta Mater.* **60** 1059
[6]   Luo ZP, Zhang HW, Hansen N and Lu K 2012 *Acta Mater.* **60** 1322
[7]   Zhang HW, Huang X and Hansen N 2008 *Acta Mater.* **56** 5451
[8]   Zhang HW, Huang X, Pippan R and Hansen N 2010 *Acta Mater.* **58** 1698
[9]   Luo ZP, Mishin OV, Zhang YB, Zhang HW and Lu K 2012 *Scripta Mater.* **66** 335
[10]   Hughes DA and Hansen N 2000 *Acta Mater.* **48** 2985
[11]   Lin FX, Zhang YB, Tao NR, Pantleon W and Juul Jensen D 2014 *Acta Mater* **72** 252
[12]   Kuhlmann-Wilsdorf D 1989 *Mater. Sci. Eng.* A **113** 1
[13]   Humphreys FJ and Hatherly M 2014 in *Recrystallization and related annealing phenomena* 2nd ed. New York: Elsvier
[14]   Murr LE 1975 *Interfacial phenomena in metals and alloys*. Addison-Wesley Publishing Company
[15]   Yu TB, Hansen N and Huang XX 2011 *Proc. Royal. Soc*. A **457** 2135
[16]   Yu TB, Hughes DA, Hansen N and Huang X 2015 *Acta Mater.* **86** 269
[17]   Li XL, Liu W, Godfrey A, Juul Jensen D and Liu Q 2007 *Acta Mater.* **55** 3531
[18]   Juul Jensen D 1995 *Acta Metall. Mater.* **43** 4117
[19]   Wang YM, Chen MW, Zhou FH and Ma E 2002 *Nature* **419** 912
[20]   Zhao YH, Zhu YT and Lavernia EJ 2010 *Adv. Eng. Mater*. **12** 759
[21]   Zhao YH, Zhu YT and Lavernia EJ 2010 *Adv. Eng. Mater*. **12** 759
[21]   Liu XC Zhang HW and Lu K 2013 *Science* **342** 337.